

# Through Silicone Vias: Multilayer interconnects for Stretchable Electronics

Joshua C. Agar, Jessica Durden, Rongwei Zhang, Daniela Staiculescu and C. P. Wong  
School of Materials Science and Engineering, Georgia Institute of Technology  
771 Ferst Drive, Atlanta, GA, 30332, USA  
Phone: 404-894-8391, Fax: 404-894-9140, E-mail: cp.wong@mse.gatech.edu

## Abstract

We show how stretchable Poly(dimethylsiloxane) (PDMS) electrically conductive composites (ECC) can be fabricated to form flexible, stretchable multilayer interconnects. Multilayer integration through via-like structures enables increased component interconnection and reduced form factor. We show a unique process for forming stretchable multilayer interconnects in PDMS via a bench-top layer-by-layer assembly technique. The SCC is reliable under bending, tensile ( $\epsilon=0.3$ ) and compressive strains. Furthermore, we show how the processes and package designs developed can be applied to the fabrication of stretchable devices. The techniques presented to fabricate ultra-low cost, stretchable, 3D packages hold the potential serve as a package for future stretchable electronic and radio frequency devices.

## Introduction

Modern consumer electronic devices are constantly striving for increased functionality and reduced form factor. The capability to produce low-cost stretchable and flexible electronic devices will enable the integration of new functionality not capable on rigid, planar substrates. For example, using bendable stretchable electronics it is possible to produce high-resolution optics [1], conformal photovoltaics [2] and large-area bio-sensor arrays [3], a feat impossible with rigid silicon electronics. However, the field of stretchable electronics is in its infancy, and the electronics packaging industry needs to adapt its technology and processes to address the new challenges associated with creating electronic devices on a stretchable, flexible platform.

Due to the poor electrical properties and reliability of solution processable active devices, first generation stretchable electronic devices will likely consist of ultra thin isolated island of active devices packaged in stretchable arrays. This design requires that the interconnects provide both electrical interconnectivity and accommodate compressive and tensile strain associated with stretching, bending and twisting [4]. Rogers et al. elegantly produces stretchable devices by interconnecting silicon active components using ultra-thin curvy metallic films mechanically transferred onto silicone [4]. However, the Rogers et al. approach is highly complex, requiring tens to hundreds of processing steps in a cleanroom environment.

A second approach to produce stretchable electrical interconnects utilizes stretchable conductive composites (SCC). SCC are typically formulated by suspending conductive fillers within a polymer matrix. Stretchable conductive polymer composites have been formulated with a wide variety of conductive fillers including, carbon black [5], carbon nanotubes [6], graphene [7], Ag nanowires [8], Ag [9, 10], etc. Typically the best conductivities are obtained when conductive composites are produced with Ag particles

because silver has the highest conductivities of all pure metals ( $6.3 \times 10^7$  S/m) and its oxide is conductive. Electrically conductive composites (ECC) with Ag fillers in epoxy matrices have resistivities on the order of  $10^{-5}$   $\Omega$ -cm [11]. However, ECC formulated in epoxy matrices are only flexible when thin and are not stretchable. Producing flexible and stretchable conductive composites requires that the composite be formulated with a highly flexible and stretchable polymeric matrix.

Silicone elastomers are the ideal matrix material for SCC. Silicone is highly stretchable, tough, chemically and thermally stable, hydrophobic and has a low toxicity. Previously we have shown that SCC with resistivity of  $7 \times 10^{-4}$   $\Omega$ -cm can be produced using a bimodal mixture of silver flakes in a silicone matrix [10].

We show how to produce highly conductive silicone conductive composites with Ag fillers and a novel additive. Furthermore, we characterize the electro-mechanical response of the produced polymer composite. Finally, we show a methodology and process to create stretchable 3D structures that could be used as a stretchable package for low cost electronic devices.

## Materials Characterization

Stretchable conductive composites (SCC) were fabricated using a silicone polymer matrix containing a bimodal distribution of silver flakes ranging in size from 1  $\mu$ m to 20  $\mu$ m (Ferro Corporation). The mixture consisted of 80:18:2 (wt%/wt%/wt%) of silver flakes, silicone (Dow Corning) and additive A respectively. The Ag flakes were dispersed in the silicone matrix using a combination of manual stirring and ultra-sonication. Two strips of Kapton tape (Dupont) were applied onto pre-cleaned glass slides. ECA was stencil printed, in-between the pieces of Kapton tape, onto the glass slides. Following thermal cure at 170°C for 30 minutes, the bulk resistance was measured using a Keithley 2000 multimeter (Keithley Instruments Inc.); using the four wire method. The width and length of the specimen was measured using a digital caliper (VWR). The thickness of the sample was measured by a Heidenhain thickness measuring equipment (ND 281B, Germany). The bulk resistivity was calculated using Eq. 1 where  $l$ ,  $w$  and  $t$  are the length, width and thickness respectively:

$$\rho = \frac{t x w}{l} R \quad (1)$$

Morphological changes in silver flakes resulting from treatment with additive A were determined by treating silver flakes with additive A at 150 °C for 15 min. Characterization of the resulting particle morphology was imaged using a LEO 1530 Scanning Electron Microscope (Carl Zeiss).

Characterization of the coefficient of thermal expansion of the conductive composite and encapsulating

Poly(dimethylsiloxane) (PDMS) was measured using a thermo-mechanical analyzer Model Q400 (TA Instruments). Dimensional changes in samples ~1 mm thick were measured as the samples were heated from room temperature to 200 °C, at a rate of 10°C/min.

A single strip of SCC was stencil printed between two strips of Kapton tape 4 mils thick onto a Pyrex wafer. SCC strips were encapsulated in PDMS by pouring degassed PDMS onto the wafer containing the SCC. The thickness of the PDMS encapsulant was controlled by weight. Following silicone cure at 60°C the samples were lifted off from the substrate using a razor blade. Dog-bone tensile specimens were cut using a razor blade, in accordance with ASTM D412 standards. The electrical response under tensile elongation was measured using a Keithley 2000 and an Instron 5548 microtester. Resistance values were recorded at 250 ms intervals during tensile elongation at an extension rate of 10 mm/sec, to a maximum elongation of 30%. We then repeated the electro-mechanical testing to tensile elongations of 30%. Finally, the electro-mechanical response of the SCC was measured until failure under tensile load.

### Fabrication of Three-Dimensional Stretchable Package

Three-dimensional (3D) stretchable packages were fabricated by spin coating Poly(methyl methacrylate) (PMMA) (Lucite International) on Pyrex wafers (Fig. 1-B). Strips of SCC were stencil printed in-between two pieces of Kapton tape 4 mils thick (Fig. 1-C). Similarly, circles of SCC 8 mm in diameter and 4 mils thick were stencil printed onto the PMMA coated Pyrex wafers using a micro-stencil (Mini Microstencil). The spacing of the circular patterns and strips had equal gap spacing such that the strips and the circular pattern could be aligned. These circular structures served as vias, interconnecting adjacent layers of SCC. Following patterning and curing of the SCC at 170 °C for 30 minutes, the SCC was encapsulated in PDMS (Fig. 1-D). The thickness of the PDMS encapsulant was controlled by weight. Following lift-off in acetone, the PDMS-encapsulated SCC was removed from the Pyrex wafer using a razor blade (Fig. 1-E). Bonding between patterned layers of SCC was accomplished by depositing a small amount of uncured SCC on the surface of the printed circular “vias” of SCC (Fig. 1-F). The PDMS-encapsulated SCC and the wafer containing the circular “vias” were bonded, at elevated pressure, at a temperature of 170°C for 30 minutes. Following curing of the SCC, PDMS was injected between the PDMS-encapsulated SCC and the Pyrex wafer containing the circular “vias” using a syringe (Fig. 1-G). The wafer was then degassed to remove air bubbles and the PDMS-encapsulant was cured at 60°C for 1 hour. The two-layer assembly was lifted off from the substrate in acetone (Fig. 1-H). This process was repeated alternating between Pyrex wafers containing the SCC strips and circular “vias”.

Electrical conductivity of the fabricated 3D interconnects was measured using the four-wire method (Keithley Instruments). Cross-sectional images of the 3D interconnects were obtained using a 3D confocal microscope (Olympus Corporation).

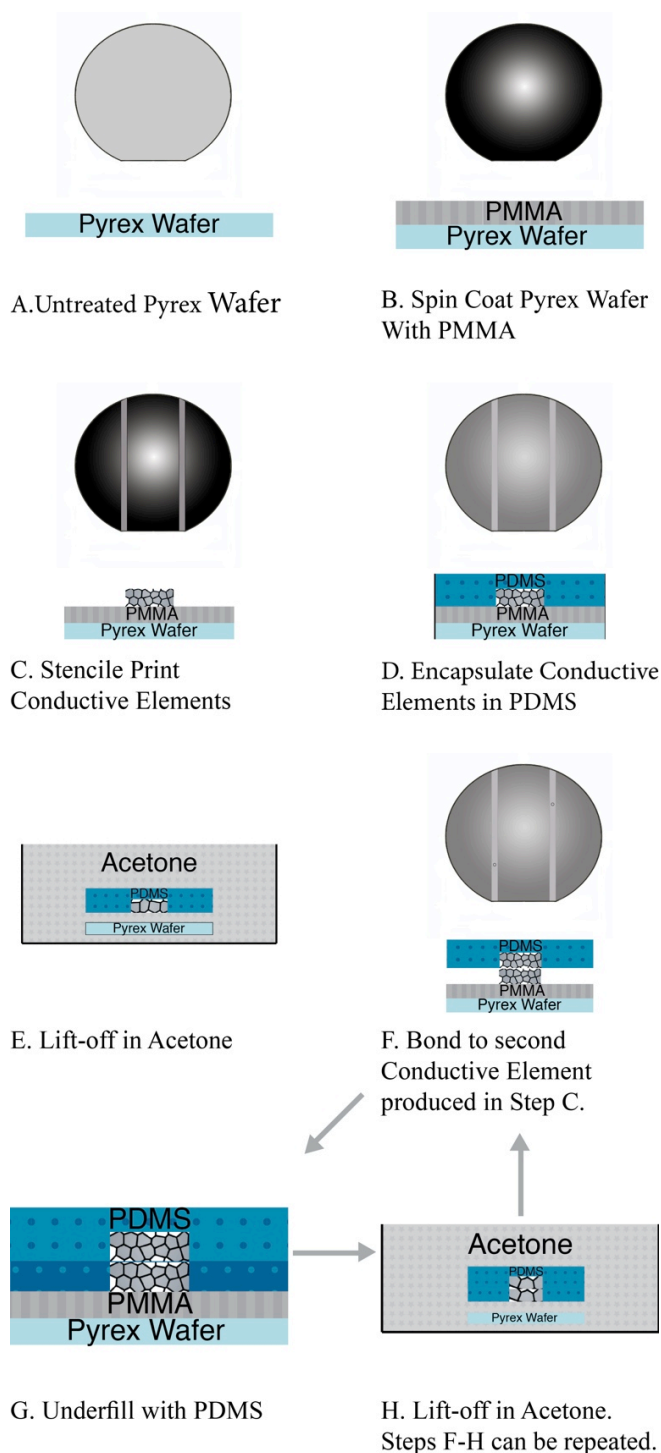


Figure 1. Schematic illustration of technique to fabricate 3D structures of SCC.

### Results:

Silicone-SCC strips were prepared as described in the experimental methods. Following curing the SCC undergoes a transition from insulating to conductive. Silicone-SCC formed with additive A had a low resistivity ( $\sim 2 \times 10^{-4} \Omega \text{ cm}$ ). This low resistivity was achieved because Additive A can reduce silver carboxylate on the surface of the silver flakes. The reduction

of silver carboxylate has two roles. First, the reduction process removes stearic acid surfactants. These surfactants are necessary for proper dispersion and to prevent aggregation of the silver flakes during mixing. However, these surfactants reduce the contact between conductive fillers. Secondly, the reduction process forms small nano/submicron-sized particles on the surface of the silver flakes. These *in-situ* formed nano/submicron particles have a high surface area to volume ratios and are not stabilized by surfactants. Thus these *in-situ* formed particles are less thermodynamically stable than pre-formed nanoparticles. The thermodynamic instability of these *in-situ* formed particles causes the particles to sinter at low temperatures ( $\sim 150^\circ\text{C}$ ). The sintering process reduces or eliminates contact resistance between flakes, enhancing the conductivity and reliability of the SCC. The effect of the addition of additive A on the morphology of the silver flakes can be seen in Fig. 2. What is important to notice in the untreated silver flakes (Fig. 2A) is the surface is smooth and the flakes appear to be stacked one on top of another. However, in the treated sample (Fig. 2B) the silver flakes have a higher surface roughness. Also, large flakes appear to be connected by small branching arms. This branching process results from the sintering of the *in-situ* formed nanoparticles. Following sintering the SCC have improved reliability and conductivity.

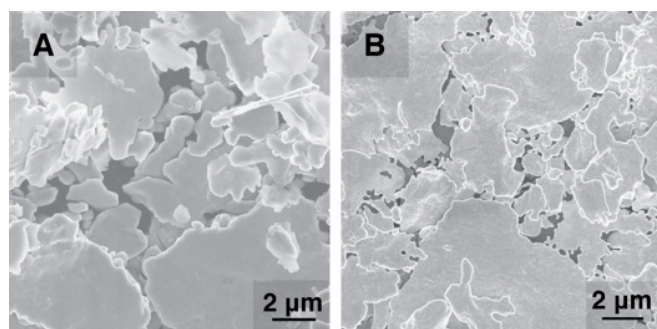


Figure 2. A. SEM image of untreated Ag flakes showing smooth surface morphology. B. SEM image of additive treated Ag flakes. Surface of Ag flakes shows rough morphology with evident sintering of *in-situ* formed Ag nanoparticles.

It is worth emphasizing that it is essential that these nanoparticles are formed *in-situ* and not just added to the formulation. The addition of pre-formed nanoparticles to composite formulations requires the nanoparticles to be stabilized with surfactants to prevent aggregation during processing. These surfactants, on pre-formed nanoparticles, stabilize the surface, reducing the driving force for sintering. Thus, conductive composites formed with pre-formed nanoparticle fillers typically have higher resistivity due to reduced contact area and thus increased contact resistance.

Prior to assembly, we characterized the linear coefficient of thermal expansion (CTE) ( $\alpha_L$ ) of both the SCC and the encapsulating PDMS using Thermo-Mechanical Analysis (TMA). A plot of the dimensional change as a function of temperature for the PDMS-encapsulant and the SCC is shown in Fig. 3. Ideally, the CTE for both the SCC and the

encapsulating PDMS should be equivalent to minimize stress at the interface and to prevent warpage. We found that the PDMS-encapsulant used had a high CTE of  $506.6 \mu\text{m}/(\text{m } ^\circ\text{C})$ . The SCC had a significantly lower CTE because it contains  $\sim 20 \text{ vol}\%$  Ag flakes with a CTE of  $\sim 18 \mu\text{m}/(\text{m } ^\circ\text{C})$ . Experimentally, we found the CTE of the SCC to be  $385.9 \mu\text{m}/(\text{m } ^\circ\text{C})$ . Even though the mismatch between these materials is large, CTE mismatch is less of a problem in stretchable electronics, compared to rigid electronics, because SCC and PDMS-encapsulant can accommodate the thermal-mechanical stresses. However, when preparing samples with a high areal density of SCC, in a non-centrosymmetric pattern, there was noticeable warpage of the layout following successive thermal cycling. The warpage associated with the CTE mismatch between the SCC and the PDMS-encapsulant will make alignment challenging, especially as feature size is reduced. In future work, it is necessary that we tailor the CTE of the PDMS-encapsulant to match the lower CTE of the SCC. This can easily be accomplished through the incorporation of fillers into the SCC matrix.

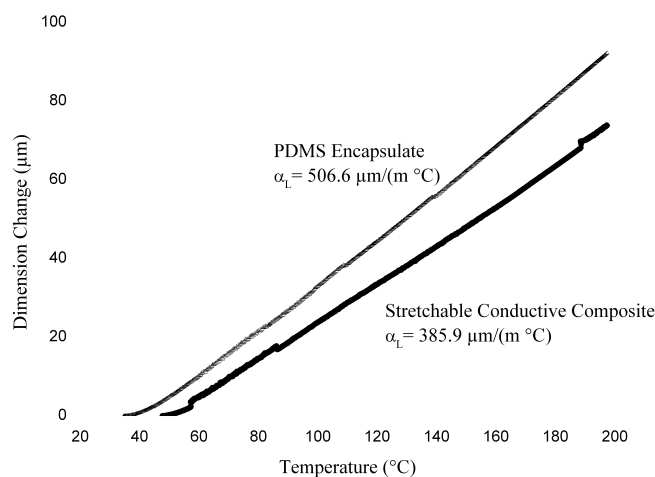


Figure 3. TMA of PDMS-encapsulate (sample size 1.161 mm) and stretchable conductive composites (sample size 1.2817 mm).

Simultaneous tensile and electrical resistance measurements were measured as described in the experimental methods. The results from these experiments are shown in Fig. 3. During the first trial the resistance of the SCC remained relatively constant up to tensile strains of  $\epsilon = 0.3$ . However, following the first tensile experiment, the tensile strain caused the anisotropic silver flakes to align. The strain induced reorganization caused the resistance of the composite to increase. However, subsequent tensile strains of  $\epsilon = 0.30$  had no additional effect on the resistance. Thus, after the initial reorganization, the composite is insensitive to repeated tensile elongation of 30%. Following repeated tensile elongations to 30%, the change in electro-mechanical response of the SCC was measured as the sample was strained to failure. The tensile-electrical measurements of the pre-strain, dog-bone specimen during strain to failure showed the resistance of the SCC initially decreased and then increased until finally failing at a strain of  $\epsilon = 0.70$ . It is worth noting that failure was

initiated in the encapsulating PDMS and not the SCC. Thus, it is likely that the composite itself could withstand tensile elongations of greater than 70% without failing.

We also manually tested the electro-mechanical response of the SCC under compression and during bending. There was significant change in the conductivity of the SCC during repeated stretching or bending.

We hypothesize two approaches to improve the electro-mechanical response of the SCC. First, we could improve the electro-mechanical response, of the SCC by incorporating high aspect ratio conductive fillers like carbon nanotubes and/or silver nanorods. A second method to improve the electro-mechanical response of the SCC would be to improve adhesion between the PDMS-encapsulant and the SCC to enhance load transfer and distribution.

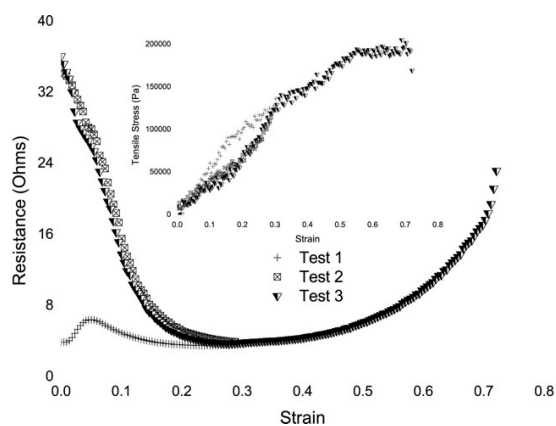


Figure 4. Graph of simultaneous tensile electro-mechanical characterization of silicone SCC. Inset: stress strain curve of dog bone tensile specimen.

As a proof of concept, we fabricated a 5-layer assembly of interconnected stretchable electrically conductive composite. A schematic drawing of the fabricated structure is shown in Figure 5.

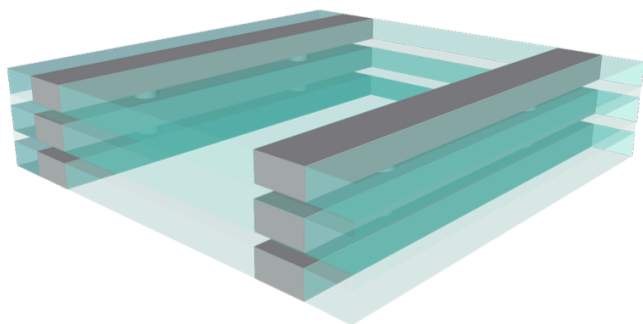


Figure 5. Schematic drawing of the fabricated a 5-layer assembly of interconnected stretchable electrically conductive composite.

Electrical characterization of the stretchable 3D conductive structures showed degradation with increasing levels of interconnection. The degradation in electrical properties associated with increased interconnection is likely the result of poor interconnection between layers. However, cross-sectional 3D confocal micrographs of the structures

showed no visual evidence of poor adhesion at the interface (Fig. 6A). Because device failure is likely to happen at the interface between two adjacent layers, it would be advantageous to use a different SCC formulation with improved adhesion and higher modulus such that the load is not accommodated by strain at the interface. Use of a different SCC formulation with improved adhesion could enhance the conductivity and reliability of the package.

Furthermore, to ensure that conductive paths on each level were isolated we took cross-sectional images using a 3D confocal micrograph. We found no evidence of inter-level connectivity other than at the “vias”. A representative cross-sectional image of the isolated levels in the 3D conductive structure is shown in Fig. 6B.

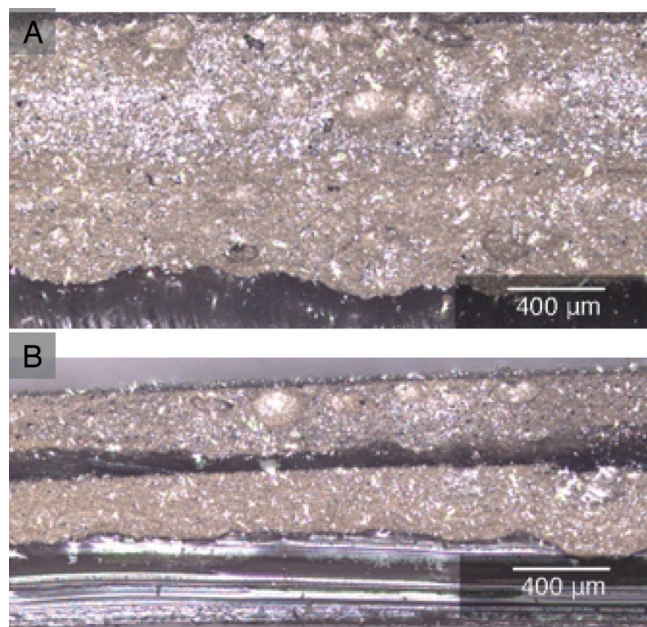


Figure 6. 3D confocal micrograph of A. Stretchable “via” like structures B. Electrically isolated layers within the stretchable conductive 3D package.

We show a method to fabricate multilayer SCC using a through silicone “via” methodology. Even though SCC are not ready for implementation in consumer devices, we show a simple, bench-top approach to fabricate 3D stretchable electrically conductive structures. This 3D stretchable package could be used to interconnect small discrete electronic devices, allowing electronic devices to be produced on a stretchable platform. Furthermore, this technology could be used succession with conventional microfluidic fabrication techniques to fabricate stretchable, solution processable, organic electronics.

Recently, we have adapted similar processing techniques to fabricate a microstrip line, a simple radio frequency (RF) device [12]. We showed that this device had good performance up to 6 GHz in a wide variety of conformations [12]. Adaptation of this technology would be useful to fabricate RF devices with improved form factor and functionally. For example, this technology could be adapted to the scientifically active fields of antennas for curvilinear

spaces [13], sensors [14] and reconfigurable antennas [15]. The ability of SCC to remove the constraints associated with rigid planar electronics holds the potential to revolutionize the interaction of electronic devices with their surroundings.

### Conclusions

We show a method to produce and package stretchable conductive silicone composites ( $\sim 2 \times 10^{-4} \Omega \text{ cm}$ ) into a 3D package. The 3D package is formed by interconnecting layers of patterned SCC with “via”-like structures of SCC. The package is mechanically robust to bending, compression and repeated tensile elongations of 30%. This design could be used to fabricate stretchable electronic devices, sensors and radio frequency devices with form factor and functionality inconceivable using conventional rigid electronic packages.

### Acknowledgments

The authors would like to acknowledge Ferro Corporation for their donation of silver flakes, Dow Corning for their donation of silicone elastomer and Lucite for their donation of PMMA. Also, I would like to acknowledge my fellow co-workers Dr. Jack Moon, Mrs. Zhuo Li, Mr. Ziyin Lin and Mr. Wei Lin for their useful insight and discussion.

### References

1. H. C. Ko, M. P. Stoykovich, J. Song, V. Malyarchuk, W. M. Choi, C.-J. Yu, J. B. Geddes Iii, J. Xiao, S. Wang, Y. Huang, and J. A. Rogers, "A hemispherical electronic eye camera based on compressible silicon optoelectronics," *Nature*, vol. 454, pp. 748-753, 2008.
2. J. Lee, J. Wu, M. Shi, J. Yoon, S.-I. Park, M. Li, Z. Liu, Y. Huang, and J. A. Rogers, "Stretchable Solar Cells: Stretchable GaAs Photovoltaics with Designs That Enable High Areal Coverage (Adv. Mater. 8/2011)," *Advanced Materials*, vol. 23, pp. 919-919, 2011.
3. D.-H. Kim, J. Viventi, J. J. Amsden, J. Xiao, L. Vigeland, Y.-S. Kim, J. A. Blanco, B. Panilaitis, E. S. Frechette, D. Contreras, D. L. Kaplan, F. G. Omenetto, Y. Huang, K.-C. Hwang, M. R. Zakin, B. Litt, and J. A. Rogers, "Dissolvable films of silk fibroin for ultrathin conformal bio-integrated electronics," *Nat Mater*, vol. 9, pp. 511-517, 2010.
4. J. A. Rogers, T. Someya, and Y. Huang, "Materials and Mechanics for Stretchable Electronics," *Science*, vol. 327, pp. 1603-1607, March 26, 2010 2010.
5. M. A. Unger, H.-P. Chou, T. Thorsen, A. Scherer, and S. R. Quake, "Monolithic Microfabricated Valves and Pumps by Multilayer Soft Lithography," *Science*, vol. 288, pp. 113-116, April 7, 2000 2000.
6. T. Sekitani, H. Nakajima, H. Maeda, T. Fukushima, T. Aida, K. Hata, and T. Someya, "Stretchable active-matrix organic light-emitting diode display using printable elastic conductors," *Nat Mater*, vol. 8, pp. 494-499, 2009.
7. M. Kujawski, J. D. Pearse, and E. Smela, "Elastomers filled with exfoliated graphite as compliant electrodes," *Carbon*, vol. 48, pp. 2409-2417, 2010.
8. Z. Yu, Q. Zhang, L. Li, Q. Chen, X. Niu, J. Liu, and Q. Pei, "Highly Flexible Silver Nanowire Electrodes for Shape-Memory Polymer Light-Emitting Diodes," *Advanced Materials*, vol. 23, pp. 664-668, 2011.
9. X. Z. Niu, S. L. Peng, L. Y. Liu, W. J. Wen, and P. Sheng, "Characterizing and Patterning of PDMS-Based Conducting Composites," *Advanced Materials*, vol. 19, pp. 2682-2686, 2007.
10. J. C. Agar, K. J. Lin, R. Zhang, J. Durden, K.-S. Moon, and C. P. Wong, "Novel PDMS(silicone)-in-PDMS(silicone): Low cost flexible electronics without metallization," in *Electronic Components and Technology Conference (ECTC), 2010 Proceedings 60th*, 2010, pp. 1226-1230.
11. R. Zhang, K.-S. Moon, W. Lin, J. C. Agar, and C.-P. Wong, "A simple, low-cost approach to prepare flexible highly conductive polymer composites by in situ reduction of silver carboxylate for flexible electronic applications," *Composites Science and Technology*, vol. 71, pp. 528-534, 2011.
12. J. Agar, J. Durden, D. Staiculescu, R. W. Zhang, E. Gebara, and C. P. Wong, "Electrically Conductive Silicone Nano-Composites For Stretchable RF Devices " in *Microwave Symposium Digest, 2011. MTT '11. IEEE MTT-S International*, 2011. (Accepted)
13. J. J. Adams, E. B. Duoss, T. F. Malkowski, M. J. Motala, B. Y. Ahn, R. G. Nuzzo, J. T. Bernhard, and J. A. Lewis, "Conformal Printing of Electrically Small Antennas on Three-Dimensional Surfaces," *Advanced Materials*, vol. 23, pp. 1335-1340, 2011.
14. B. Y. Lee, K. Heo, J. H. Bak, S. U. Cho, S. Moon, Y. D. Park, and S. Hong, "Scalable Assembly Method of Vertically-Suspended and Stretched Carbon Nanotube Network Devices for Nanoscale Electro-Mechanical Sensing Components," *Nano Letters*, vol. 8, pp. 4483-4487, 2008.
15. C. Shi, W. Zhigang, P. Hallbjorner, K. Hjort, and A. Rydberg, "Foldable and Stretchable Liquid Metal Planar Inverted Cone Antenna," *Antennas and Propagation, IEEE Transactions on*, vol. 57, pp. 3765-3771, 2009.